A Role for Monomethylation of Histone H3-K27 in Gene Activity in *Drosophila*

Liangjun Wang,* Preeti Joshi,* Ellen L. Miller,* LeeAnn Higgins,† Matthew Slattery,‡ and Jeffrey A. Simon*,[1]

*Department of Genetics, Cell Biology and Development and †Department of Biochemistry, Molecular Biology and Biophysics, University of Minnesota, Minneapolis, Minnesota 55455 and ‡Department of Biomedical Sciences, University of Minnesota Medical School, Duluth, Minnesota 55812

ABSTRACT Polycomb repressive complex 2 (PRC2) is a conserved chromatin-modifying enzyme that methylates histone H3 on lysine-27 (K27). PRC2 can add one, two, or three methyl groups and the fully methylated product, H3-K27me3, is a hallmark of Polycomb-silenced chromatin. Less is known about functions of K27me1 and K27me2 and the dynamics of flux through these states. These modifications could serve mainly as intermediates to produce K27me3 or they could each convey distinct epigenetic information. To investigate this, we engineered a variant of *Drosophila melanogaster* PRC2 which is converted into a monomethyltransferase. A single substitution, F738Y, in the lysine-substrate binding pocket of the catalytic subunit, E(Z), creates an enzyme that retains robust K27 monomethylation but dramatically reduced di- and trimethylation. Overexpression of E(Z)-F738Y in fly cells triggers desilencing of Polycomb target genes significantly more than comparable overexpression of catalytically deficient E(Z), suggesting that H3-K27me1 contributes positively to gene activity. Consistent with this, normal genomic distribution of H3-K27me1 is enriched on actively transcribed *Drosophila* genes, with localization overlapping the active H3-K36me2/3 chromatin marks. Thus, distinct K27 methylation states link to either repression or activation depending upon the number of added methyl groups. If so, then H3-K27me1 deposition may involve alternative methyltransferases beyond PRC2, which is primarily repressive. Indeed, assays on fly embryos with PRC2 genetically inactivated, and on fly cells with PRC2 chemically inhibited, show that substantial H3-K27me1 accumulates independently of PRC2. These findings imply distinct roles for K27me1 *vs.* K27me3 in transcriptional control and an expanded machinery for methylating H3-K27.

KEYWORDS chromatin; transcription; Polycomb; epigenetics; gene silencing

COVALENT histone modifications such as methylation, acetylation, phosphorylation, and ubiquitylation are widespread in eukaryotic genomes, where they impact diverse chromatin processes including transcription, DNA replication and repair, and mitotic progression (Bannister and Kouzarides 2011; Zentner and Henikoff 2013). This large spectrum of histone modifications creates great diversity in chromatin landscapes. Since implementers and modulators of chromatin processes can read these modifications via direct biochemical contact (Taverna *et al.* 2007), their many combinations provide an array of potential regulatory levers and buttons. For histone methylation, this complexity is expanded by the possibility of three distinct states at each modified residue. Specifically, arginine (R) can be monomethylated, symmetrically dimethylated, or asymmetrically dimethylated and lysine (K) can be mono-, di-, or trimethylated (Klose and Zhang 2007). Each alternative state has potentially distinct functional impacts, reflecting altered affinities or influences upon chromatin factors that recognize them.

Although precise mechanistic consequences of many histone modifications are yet to be determined, general insights have emerged from studies on the responsible enzymes and from extensive epigenomic analyses. Methylation of histone H3 on lysine-4 (H3-K4me) and lysine-36 (H3-K36me) are associated with gene activity, whereas H3-K9me and H3-K27me often mark transcriptionally silent or low-activity loci. Importantly, genome-wide analyses reveal that different

doi: https://doi.org/10.1534/genetics.117.300585
Manuscript received July 20, 2017; accepted for publication December 7, 2017; published Early Online December 14, 2017.
Supplemental material is available online at www.genetics.org/lookup/suppl/doi:10.1534/genetics.117.300585/-/DC1.
[1]Corresponding author: Department of Genetics, Cell Biology and Development, University of Minnesota, 321 Church St. SE, Minneapolis, MN 55455. E-mail: simon004@umn.edu

methylation states at these key lysines are linked to distinct roles in transcription. For example, H3-K4me3 is a common feature at active gene promoters (Heintzman *et al.* 2007; Kharchenko *et al.* 2011) whereas H3-K4me1 forms part of the chromatin signature at enhancers (Heintzman *et al.* 2009; Creyghton *et al.* 2010; Rada-Iglesias *et al.* 2011; Herz *et al.* 2012). Similarly, although H3-K36 methylation is generally associated with active gene bodies (Barski *et al.* 2007; Barrand *et al.* 2010; Kharchenko *et al.* 2011), there are distinct peak distributions: K36me1 predominates in 5′ regions, K36me2 is most abundant in midgene locations, and K36me3 is highest at 3′ ends (Bell *et al.* 2007; Venkatesh and Workman 2013). These differential distributions imply that functional roles and molecular interactions are altered by the mere addition of one or two methyl groups.

One of the most extensively studied histone modifications, H3-K27me3, is a hallmark of Polycomb silencing (Margueron and Reinberg 2011; Simon and Kingston 2013). The enzyme responsible for K27 trimethylation, PRC2, is present in single-celled eukaryotes and fungal species and is highly conserved in plants and animals (Sawarkar and Paro 2010), where it is centrally integrated into stem cell transcriptional programs (Pereira *et al.* 2010; Surface *et al.* 2010; Xie *et al.* 2014). Although H3-K27me3 is fundamentally associated with developmental gene silencing, its mechanistic consequences are not completely understood. Importantly, analyses of histone H3 mutants in *Drosophila* imply that K27 methylation has a causative rather than passive role in transcription decisions (Pengelly *et al.* 2013; McKay *et al.* 2015). Furthermore, altered H3-K27 methylation resulting from PRC2 subunit mutation or H3-K27M substitution is implicated as a driver in certain lymphomas (McCabe *et al.* 2012; Kim and Roberts 2016) and glioblastomas (Chan *et al.* 2013; Lewis *et al.* 2013), and PRC2 subunit overabundance is linked to many types of solid tumors (Simon and Lange 2008; Kim and Roberts 2016). These findings underscore the critical role of H3-K27me3 in setting and reprogramming genome expression profiles during both normal development and disease.

The importance of H3-K27me3 in eukaryotic genomes raises questions about alternative K27 methylation states. Are K27me1 and K27me2 merely neutral steps on the path to repressive K27me3 or do they each convey distinct epigenetic functions? An original study, using *Drosophila* polytene chromosome immunostaining (Ebert *et al.* 2004), found that K27me1 and K27me2 are widespread, with both decorating much of the euchromatic genome. In contrast, K27me3 is much more limited, with signal detected mainly at ~100 discrete sites corresponding to Polycomb targets such as *Hox* loci. Since the patterns were clearly not coincident, these distributions suggest that K27me1 and K27me2 are not just intermediates toward building K27me3. However, functional consequences at the many sites that harbor K27me1 and/or K27me2 have not been defined.

Subsequent analyses of H3-K27me1 genomic distributions, in a wide spectrum of plant and animal species, supplies further clues about potential functions. However, different outcomes have been observed among different classes of organisms. In mammalian cells, the bulk of evidence correlates K27me1 distribution with active genes (Barski *et al.* 2007; Wang *et al.* 2008; Ernst and Kellis 2010; Ferrari *et al.* 2014). Most of these studies detect K27me1 enrichment within gene bodies, suggesting a cotranscriptional role. Enrichment at mammalian gene enhancers and promoters has also been described (Cui *et al.* 2009; Ernst and Kellis 2010; Steiner *et al.* 2011). In *Caenorhabditis elegans*, K27me1 is coassociated with dosage compensation proteins that mediate X-linked gene repression (Liu *et al.* 2011b). However, depending upon worm developmental stage, K27me1 was coenriched with features of either silent or active chromatin. This is clearly distinct from K27me3, which is highly coincident with repressed chromatin in *C. elegans* (Liu *et al.* 2011b). In plants, K27me1 is mainly linked to heterochromatin (Jacob *et al.* 2009; Roudier *et al.* 2011; Baker *et al.* 2015), which implies a primary role in silent chromatin. Thus, K27me1 has been linked to either gene activity or silencing, depending upon developmental stage and species assayed.

Here we sought to address potential K27me1 functions via further analyses using *Drosophila*. We report that K27me1 genomic distribution in *Drosophila* cells resembles its distribution in mammalian cell types, with clear enrichment in transcriptionally active regions. We also developed tools to manipulate K27me1 abundance to enable investigation of its functional consequences in target chromatin. Specifically, we engineered a PRC2 variant with dramatically elevated K27 monomethylation activity, and harnessed this tool to track changes in target gene output when local K27me1 density is boosted. Our findings suggest that K27me1 exerts a positive influence on transcriptional activity. We also exploit genetic and chemical tools that impair PRC2 activity to reveal that a substantial fraction of K27me1 modification in *Drosophila* may be delivered by enzymes other than PRC2.

Materials and Methods

Determination of methylation state distributions from genome-wide data

Genome-wide chromatin immunoprecipitation (ChIP) enrichment data were downloaded from the modENCODE repository (http://data.modencode.org). All data represent ChIP-chip experiments performed with chromatin from S2 cells. The following modENCODE IDs were used: 298 (K27me3), 303 (K36me3), 305 (K4me3), 3000 (K27me2), and 3943 (K27me1). RNA-sequencing data from modENCODE was used to identify genes highly expressed and genes not expressed in S2 cells; see Table S3 in Cherbas *et al.* (2011) for reads per kilobase of transcript per million mapped reads (RPKM) values. Genes with RPKM $>$ 50 were considered highly expressed, and genes with RPKM $=$ 0 were called as not expressed. Metagene plots, with partitioning by highly expressed and unexpressed genes, were generated using the *cis*-regulatory element annotation system as part of the

Cistrome platform (Shin *et al.* 2009; Liu *et al.* 2011a). Pearson correlation coefficients for all ChIP data were also calculated in Cistrome (Liu *et al.* 2011a), using average enrichment signals for 1 kb windows across the whole genome.

Baculovirus expression and purification of recombinant PRC2 complexes

Baculovirus expression of recombinant proteins in insect Sf9 cells was performed using the Bac-to-Bac system (Thermo Fisher Scientific). Full-length complementary DNAs encoding FLAG-ESC, E(Z), SU(Z)12, and NURF55 inserted into pFastBac1 were obtained as described (Muller *et al.* 2002; Ketel *et al.* 2005). Site-directed E(Z) mutations were generated using the QuikChange Mutagenesis kit (Agilent Technologies) and were sequenced to confirm intact coding regions. Anti-FLAG immunoaffinity purification of PRC2 complexes was performed as described (Ketel *et al.* 2005; Joshi *et al.* 2008), with washes of resin-bound PRC2 containing up to 1.2 M potassium chloride. Mutant complexes were routinely prepared in parallel with a wild-type control, and purified at least twice independently for each complex.

Histone methyltransferase assays

Histone methyltransferase (HMTase) assays on mutant PRC2 complexes (Figure 2C) were performed as described (Rai *et al.* 2013), and were repeated at least twice using independent preparations of mutant PRC2. Histone content was visualized by Amido Black staining. HMTase quantitation was performed by scintillation counting of excised histone bands. HMTase reactions using ^{3}H-S-adenosylmethionine (SAM) were performed for 1 hr at 30°. Reactions with nonradioactive SAM were performed for 18 hr at 30° with 300 μM SAM (Figure 3, B and C), or for 1 hr at 30° with either 3 or 30 μM SAM (Supplemental Material, Figure S5B). Polynucleosome substrate, consisting of 8–12 mers purified from HeLa cells, was prepared as described (Ketel *et al.* 2005) and used at 60 ng/μl. *Drosophila* H3/H4 tetramers were prepared after coexpression of histones H3 and H4 in *Escherichia coli* (Levenstein and Kadonaga 2002) and used at 15 ng/μl.

Antibodies, Western blots, and co- immunoprecipitations

Protein extracts from fly S2 cells were prepared as described (Wang *et al.* 2004), and were fractionated on 10% SDS-PAGE gels for Western blot analysis. Blots were incubated with primary antibodies anti-HA (Cell Signaling Technology) at 1:1000, anti-E(Z) (Carrington and Jones 1996) at 1:100, and anti-tubulin (Sigma, St. Louis, MO) at 1:2500 as lane loading control. Histones were acid-extracted from S2 cells or from fly embryos using the EpiQuick kit (Epigentek) and histone extracts, or H3/H4 tetramers (Figure 3B), were fractionated on 15% SDS-PAGE gels and transferred to Protran (Schleicher & Schuell, Keene, NH) for Western blotting. Histone modifications were detected with anti-H3K27me1 (Epigentek) at 1:1000, anti-H3K27me2 (Millipore, Bedford, MA) at 1:1000, and anti-H3K27Me3 (Millipore) at 1:1000 (Figure 3B and Figure 4A) or anti-H3K27Me3 (Cell Signaling Technology) at 1:1000 (Figure 6, A and C, Figure S5B, and Figure S6A). Loading controls on histone blots were performed using anti-H3 (Millipore) at 1:500 (Figure 3B) or anti-H4 (Abcam) at 1:2000. Immunoprecipitations on S2 cell extracts were performed as described (Jones *et al.* 1998; Wang *et al.* 2006), using 10 μl of anti-SU(Z)12 (Muller *et al.* 2002) and anti-HA (see above) to detect associated HA-E(Z).

S2 cell transfections, ChIPs, and RT- PCR

Transfection constructs were built with the pAc5.1 vector (Invitrogen, Carlsbad, CA) to express E(Z) transgenes from an actin promoter. S2 cell transfections were performed as described (Rai *et al.* 2013), except S2 cells were transfected twice, on days 1 and 4 of culture, prior to harvesting for assays on day 7. ChIP assays were performed as described (Wang *et al.* 2010), using 5 μl anti-H3K27me1 (Active Motif), 5 μl anti-H3K27Ac (Active Motif), or 5 μl anti-H3K27me3 (Cell Signaling Technology). RT-PCR was performed using total RNA extracted from S2 cells using TRIzol reagent (Invitrogen). Reverse transcription was performed as described (Wang *et al.* 2010). Briefly, complementary DNA was synthesized from total RNA and random primers using SuperscriptII (Invitrogen). Real-time quantitative PCR (Q-PCR) was carried out in a 10 μl volume using Platinum SYBR green qPCR SuperMix-UDG (Invitrogen). Q-PCR was performed using 45 cycles consisting of 95° for 30 sec, 50° for 30 sec, and 72° for 30 sec on a Mastercycler RealPlex 2S (Eppendorf). RpII140 was used as an internal control.

PRC2 inhibitor assays and RNA interference in S2 cells

Aliquots of 2×10^6 fly S2 cells were treated twice with 10 μM EZH2 inhibitor EPZ6438 (Knutson *et al.* 2013) over a 7-day period, with inhibitor administered on the first and fourth days of culture. Cells were then harvested and histones were acid-extracted using the EpiQuick kit (Epigentek), before subjecting to Western blot analyses (see above) to track H3-K27 methylation states. E(Z) RNA interference was performed as described (Wang *et al.* 2004).

Mass spectrometry

HMTase reactions using nonradioactive SAM, and matrix-assisted laser desorption/ionization (MALDI) mass spectrometric analysis of resulting H3-K27 products (Figure 3C), were performed as described (Joshi *et al.* 2008), using an AB SCIEX 4800 MALDI TOF/TOF analyzer (Sciex, Framingham, MA). Spectral counting was performed as follows. Total histones were acid-extracted from wild-type and *esc* mutant fly embryos (0–24 hr) using the EpiQuick kit (Epigentek). Production of *esc* mutant fly embryos, as the progeny of esc^{10} *b pr*/esc^{2} *Cy0* adults, was as described (Ketel *et al.* 2005). esc^{10} is a 380-kb deficiency that removes the *esc* locus, and esc^{2} is an apparent null allele resulting from a frameshift (Struhl 1981; Frei *et al.* 1985; Sathe and Harte 1995). Two micrograms of acid-extracted proteins were resolved on 15% SDS-PAGE gels and stained with Coomassie Blue. Histone H3

bands were excised, destained, treated with propionic anhydride, digested with trypsin, and resulting peptides were eluted as described (Joshi *et al.* 2008). After purification via C18 resin using the "Stage Tip" protocol (Rappsilber *et al.* 2003), one 50th of total samples were analyzed on an LTQ Orbitrap Velos (Thermo Scientific) instrument essentially as described (Lin-Moshier *et al.* 2013). PEAKS 7.5 software (Bioinformatics Solutions) was used to search the *Drosophila* protein FASTA database, with cross-checking against the common laboratory contaminants database at http://www.thegpm.org/crap. Numbers of tandem mass spectra corresponding to H3/H3.3 peptides spanning amino acid residues 27–40 (aa27–40) and bearing K27 methylation(s) or acetylation were counted. Relative abundance of modification states (Figure 6B) represents the number of aa27–40 spectra indicative of K27me0, K27me1, K27me2, or K27me3, divided by the total number of aa27–40 spectra.

Data availability

The authors state that all data necessary for confirming the conclusions presented in the article are represented fully within the article.

Results

Enrichment of H3-K27me1 on active genes in Drosophila

To investigate potential functions of H3-K27me1 in *Drosophila*, we began by analyzing its genome-wide distributions in datasets compiled from fly cells relative to the transcriptome (http://data.modencode.org). Figure 1A shows metagene profiles that compare the three possible K27 methylation states in cultured *Drosophila* S2 cells. Whereas K27me2 and K27me3 distributions are highly correlated with repressed genes, K27me1 is instead preferentially enriched at active gene loci. When compared with canonical marks of active transcription, namely promoter-enriched H3-K4me3 and gene body–enriched H3-K36me3 (bottom two panels), K27me1 more closely tracks with the cotranscriptional distribution of K36me3, including its characteristic increase toward the 3′ ends of genes. When plots are instead centered at transcription start sites (Figure S1), promoter-associated K4me3 is emphasized, as expected, and the distinct coenrichment of K27me1 with K36me3 along downstream gene bodies is again apparent. Indeed, K27me1 displays substantial overall genome-wide correlation with K36me3 (0.66; Figure 1B). These findings suggest an active role for K27me1 in transcription, rather than a neutral entity used merely to build repressive K27me3. This enrichment pattern resembles findings from mammalian cells; for example, the genome-wide distribution of K27me1 in mouse embryonic stem cells is also highly correlated with gene activity rather than silencing (Ferrari *et al.* 2014).

Engineering an F-to-Y switch in the catalytic domain of PRC2

To investigate functional consequences of altered K27me1 levels in cells, we sought to modify PRC2 enzyme function so

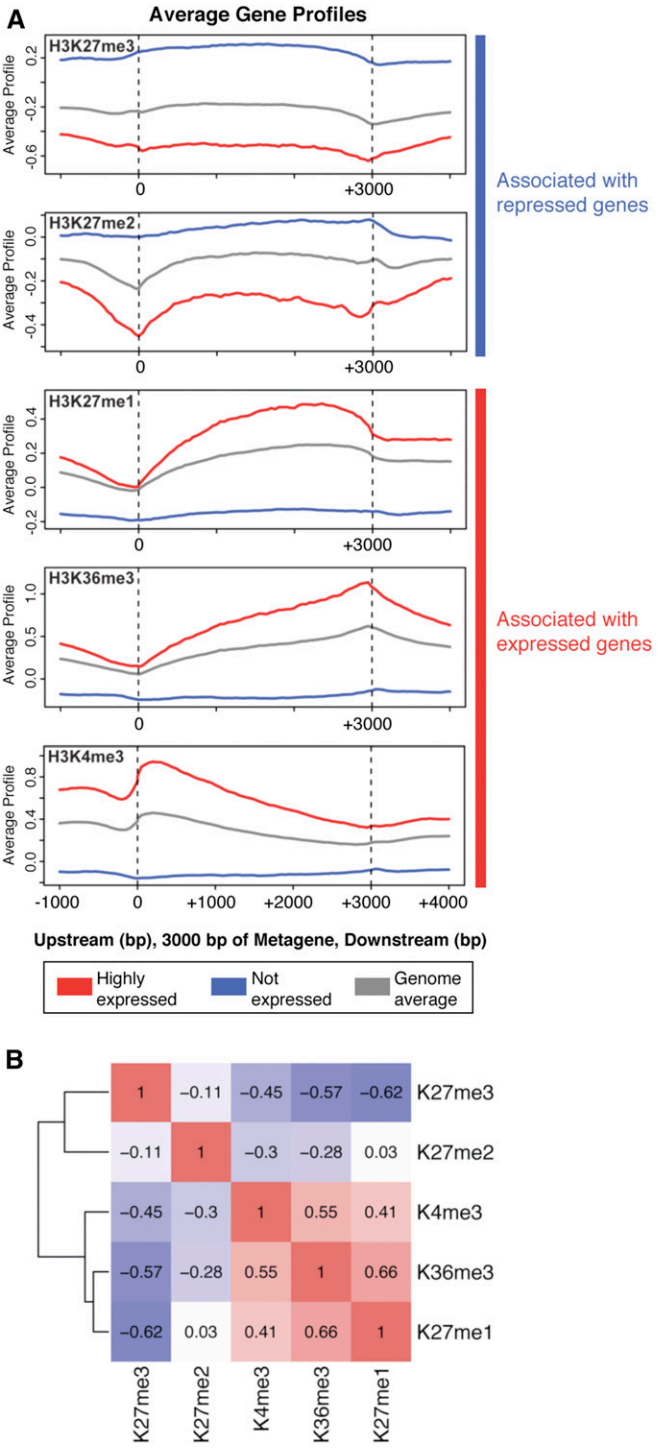

Figure 1 Distributions of select histone H3 methylation states in *Drosophila* S2 cells. (A) Metagene profiles derived from genome-wide histone modification ChIP data (http://data.modencode.org). Profiles for H3-K27me1, H3-K27me2, and H3-K27me3 are displayed along with profiles for the active marks H3-K36me3 and H3-K4me3. Average signal across all genes is represented in gray, average signal across highly expressed genes is in red, and average signal across unexpressed genes is in blue. (B) Genome-wide Pearson correlation coefficients for the five indicated histone modifications. K27me1 is positively correlated with active gene-associated histone methylation marks.

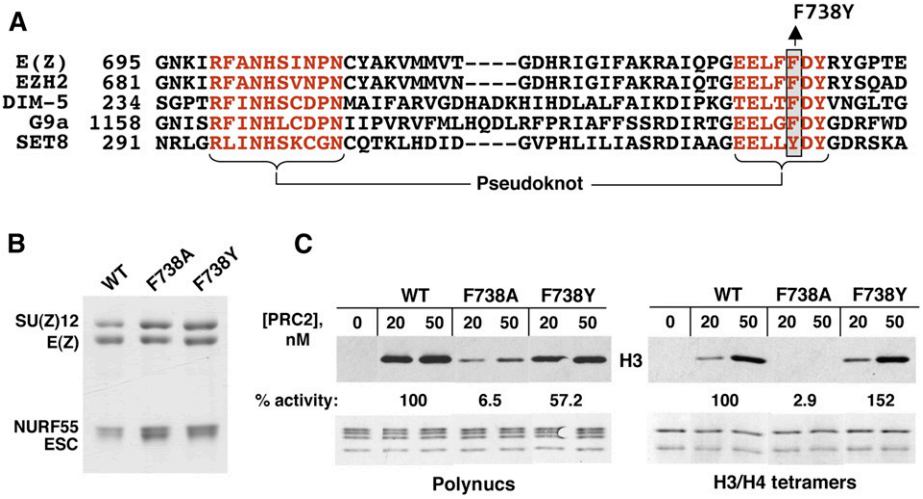

Figure 2 Engineering an F-to-Y switch in PRC2 to alter methylation capacity. (A) Location of key residues that impact methylation multiplicity in SET domain methyltransferases. F-to-Y switches have previously been described for DIM-5, G9a, and SET8 (Zhang *et al.* 2003; Collins *et al.* 2005; Couture *et al.* 2008). (B) Assembly of indicated mutant versions of E(Z) into recombinant four-subunit PRC2. (C) HMTase activities of PRC2 bearing indicated F738 mutations. Top panels show HMTase assays and bottom panels show Coomassie Blue gels of the substrates used (HeLa polynucleosomes on left and recombinant H3/H4 tetramers on right).

that its K27 methylation activity is restricted to monomethylation. This could provide a tool to create elevated levels of H3-K27me1 at normal PRC2 target genes. Prior work on HMTases that target H3-K4, H3-K9, or H4-K20 identified particular aromatic residues within the catalytic SET domain that govern methylation multiplicity (Zhang *et al.* 2003; Collins *et al.* 2005; Couture *et al.* 2005, 2008). Specifically, presence of a phenylalanine (F) residue at a key position in the lysine-substrate binding pocket (Figure 2A) supports mono-, di-, and trimethylation, whereas occurrence of tyrosine (Y) at this position can restrict activity to monomethylation. Thus, monomethylation *vs.* di- and trimethylation capacity can be toggled by targeted substitution, a process referred to as the F-to-Y switch (Collins *et al.* 2005).

Wild-type fly E(Z) bears F738 at this key position and, when assembled into recombinant PRC2, is fully capable of all three methyl transfer reactions to ultimately produce K27me3 from a K27me0 substrate (Nekrasov *et al.* 2007; Joshi *et al.* 2008). Based on successful F-to-Y switch engineering in DIM-5, G9a, and SET8 (Zhang *et al.* 2003; Collins *et al.* 2005; Couture *et al.* 2005, 2008) at the comparable position (Figure 2A), we constructed an E(Z) mutant bearing F738Y. We also constructed F738A, which should disrupt all HMTase activity and thereby serve as a key comparative control. Figure 2B shows that E(Z) bearing either F738Y or F738A retains the ability to assemble into PRC2, like wild type. Encouragingly, HMTase assays, using either HeLa polynucleosomes or unmodified H3/H4 tetramers as substrate, show that PRC2 bearing F738Y retains robust histone methylation activity, whereas the F738A version is dramatically impaired (Figure 2C).

E(Z)-F738Y converts PRC2 into a monomethyltransferase

To determine if E(Z)-F738Y alters methylation output, we analyzed HMTase reaction products generated by recombinant four-subunit PRC2 bearing this substitution (Figure 3A). The substrate used was H3/H4 tetramers produced in *E. coli*, which are unmodified at K27 upon isolation (Figure 3B, right lane and Figure 3C, upper left). Western blot analyses of reaction products are shown in Figure 3B. The negative control, F738A, shows dramatically reduced accumulation of all K27-methylated species, as expected. As a positive control, we used E(Z)-F679Y, a different F-to-Y mutant which we previously found to retain trimethylation activity (Joshi *et al.* 2008). Under these reaction conditions, both wild-type PRC2 and the F679Y control produce readily detectable amounts of K27me1, K27me2, and K27me3 from the K27me0 substrate. In contrast, PRC2-F738Y produces elevated amounts of K27me1 but comparatively little K27me2 or K27me3 (Figure 3B, lane 4).

To assess methylation capacity using an antibody-independent method, we analyzed the products of similar HMTase reactions by MALDI mass spectrometry. Figure 3C shows mass spectra of the H3 peptide spanning residues aa27–40, produced by tryptic cleavage after propionylation (Peters *et al.* 2003). The results confirm that PRC2-F738Y primarily generates K27me1 (Figure 3C, red arrow, lower right panel) whereas wild-type PRC2 and the F679Y positive control produce all three methylation products. Thus, under these conditions, wild-type PRC2 enacts successive methyl transfers to ultimately yield K27me3, whereas PRC2-F738Y activity is mainly limited to production of K27me1. We conclude that incorporation of E(Z)-F738Y converts recombinant PRC2 into a monomethyltransferase *in vitro*.

Overexpression of E(Z)-F738Y boosts H3-K27me1 in fly cells

To investigate impact of this monomethylating PRC2 in a cellular context, we overexpressed E(Z)-F738Y in fly S2 cells via transfection and then assayed consequences upon chromatin state and transcriptional outputs. Comparison of transfected *vs.* mock-treated cell samples routinely yielded a several-fold increase in overall E(Z) above endogenous levels (Figure 4A). In these and following experiments, cells expressing HA-tagged versions of wild-type E(Z), monomethylating E(Z)-F738Y, and enzyme-deficient E(Z)-F738A were assayed in parallel, with comparable accumulations of exogenous E(Z) monitored by anti-HA Western blot. Co-immunoprecipitations on extracts from transfected cells confirmed association of exogenous E(Z) with endogenous

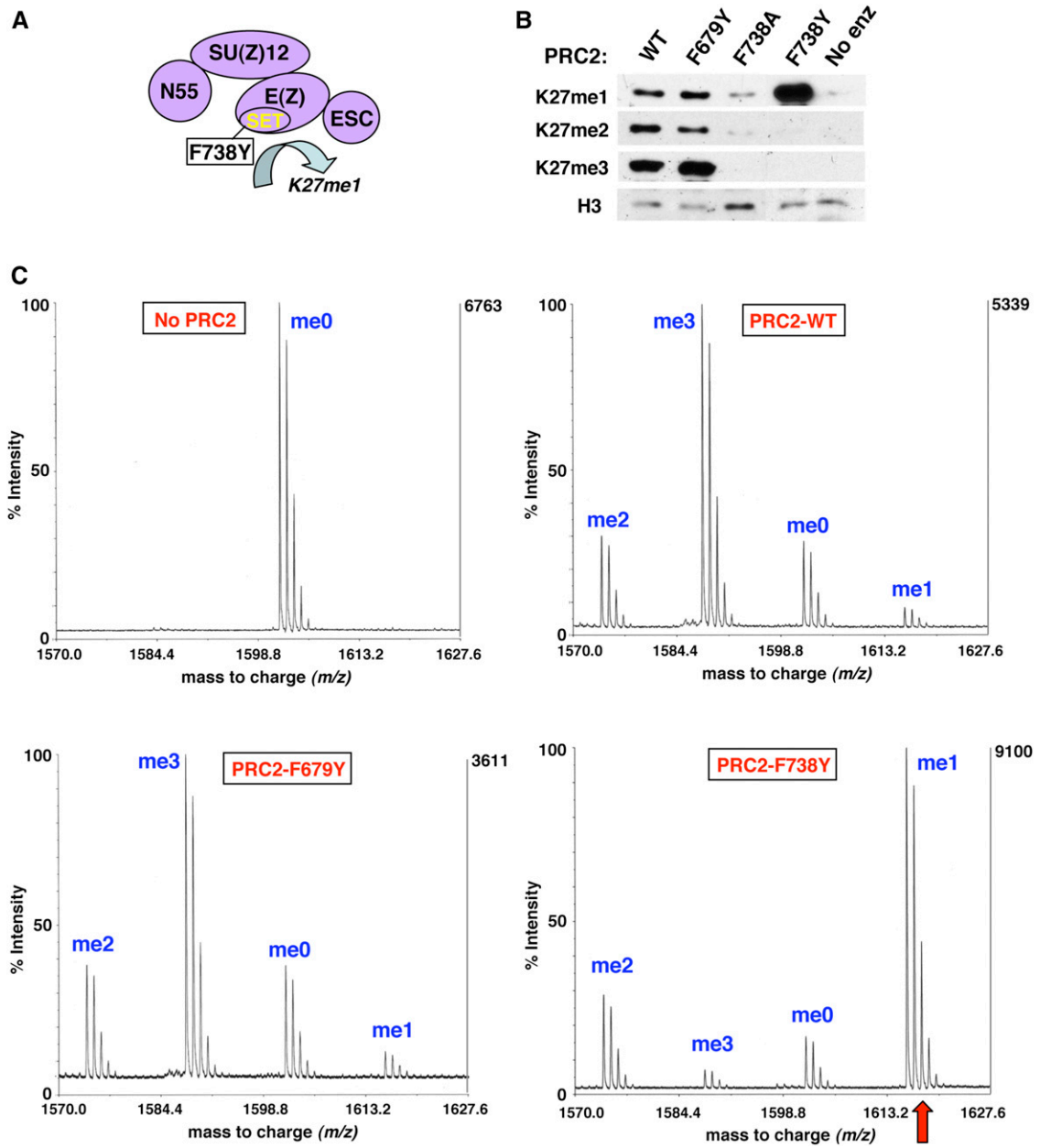

Figure 3 PRC2 bearing E(Z)-F738Y is converted into a monomethylating enzyme. (A) Cartoon depicting PRC2 reengineered into a monomethyltransferase. (B) Western blots on *in vitro*-generated HMTase reaction products to track methylation outputs. The methylation state-specific or pan-H3 antibodies used are indicated on the left and mutant forms of PRC2 are indicated at the top. WT indicates wild type and No enz indicates a mock reaction with PRC2 omitted. (C) MALDI mass spectrometric analyses of HMTase reaction products produced by *in vitro* treatment of recombinant *Drosophila* H3/H4 tetramers with indicated forms of PRC2. Detection of the indicated unmodified and K27-methylated forms of histone H3 tail tryptic peptide aa27–40 (KSAPATGGVKKPHR), was performed as described (Peters *et al.* 2003; see *Materials and Methods*). Red arrow indicates the predominant K27me1 peak obtained with PRC2 bearing E(Z)-F738Y.

SU(Z)12 (Figure 4B and Figure S2A), implying that the altered versions of E(Z) can assemble into PRC2 in cells.

To determine if excess E(Z)-F738Y alters H3-K27 methylation status in the transfected cells, we first analyzed bulk chromatin by Western blot (Figure 4A, bottom). These assays revealed that the balance of methylation states is shifted toward K27me1 in the E(Z)-F738Y-transfected cells (red arrow). In contrast, E(Z)-F738A-expressing cells showed a decline in all K27 methylation states, consistent with general dominant-negative interference with PRC2 activity. To assess consequences at a defined target gene, we performed ChIP to track K27me1 at several locations along the Hox gene *Ubx* (Figure 4C). We found that K27me1 levels were significantly elevated in E(Z)-F738Y-expressing cells compared with cells transfected to express F738A or wild-type E(Z) (Figure 4D). Elevated K27me1 was detected across a broad swath of the *Ubx* gene, spanning the upstream regulatory region, the promoter region, and the coding region. These results suggest

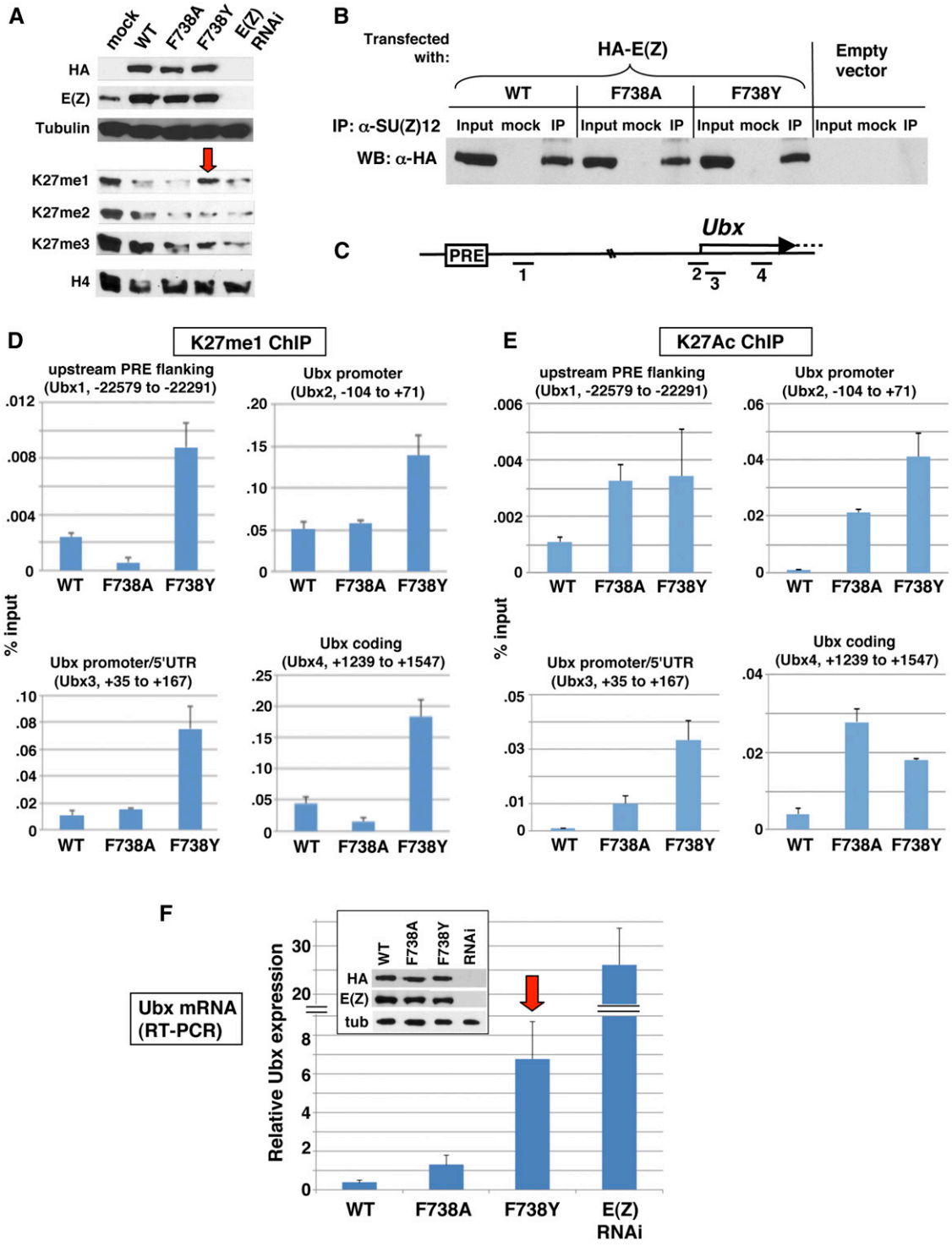

Figure 4 Impacts of E(Z)-F738Y in *Drosophila* S2 cells. (A) Western blots to track expression of transfected forms of HA-tagged E(Z) (top) and resulting methylation status (bottom) in S2 cells. mock indicates cells transfected with empty vector. Red arrow denotes increase in bulk K27me1 level as compared to other K27 methylation states. (B) Co-immunoprecipitation of exogenous E(Z) with endogenous SU(Z)12. Cells were transfected with indicated form of HA-E(Z), resulting extracts immunoprecipitated with anti-SU(Z)12 antibody, and then probed with anti-HA. mock denotes IP without anti-SU(Z)12 (protein A-agarose alone). (C) Cartoon depicts 5′ portions of the *Ubx* gene, including the transcription start region and a PRE located ~25 kb upstream within the *bxd* regulatory region. Fragments 1–4 represent amplicons used in ChIP assays. Fragment 1 is located ~2 kb from the PRE. Map is not drawn precisely to scale. (D) ChIP to track H3-K27me1 on the target gene *Ubx* after transfection with indicated forms of HA-E(Z). Graphs display four tested locations, numbered in base pairs relative to transcription start site, and corresponding to the amplicons shown in (C). (E) ChIP to track H3-K27Ac at the same four locations tested in (D) and displayed in (C). (F) RT-PCR to track changes in *Ubx* mRNA levels. Inset shows Western blot verifying comparable levels of exogenous E(Z) in the transfected cells. Red arrow emphasizes *Ubx* desilencing observed in F738Y sample (as compared to F738A sample). In (A) and (F), E(Z) RNAi denotes cells treated with double-stranded RNA to reduce E(Z) levels. In (D)–(F), error bars denote SEM from Q-PCR reactions performed in triplicate.

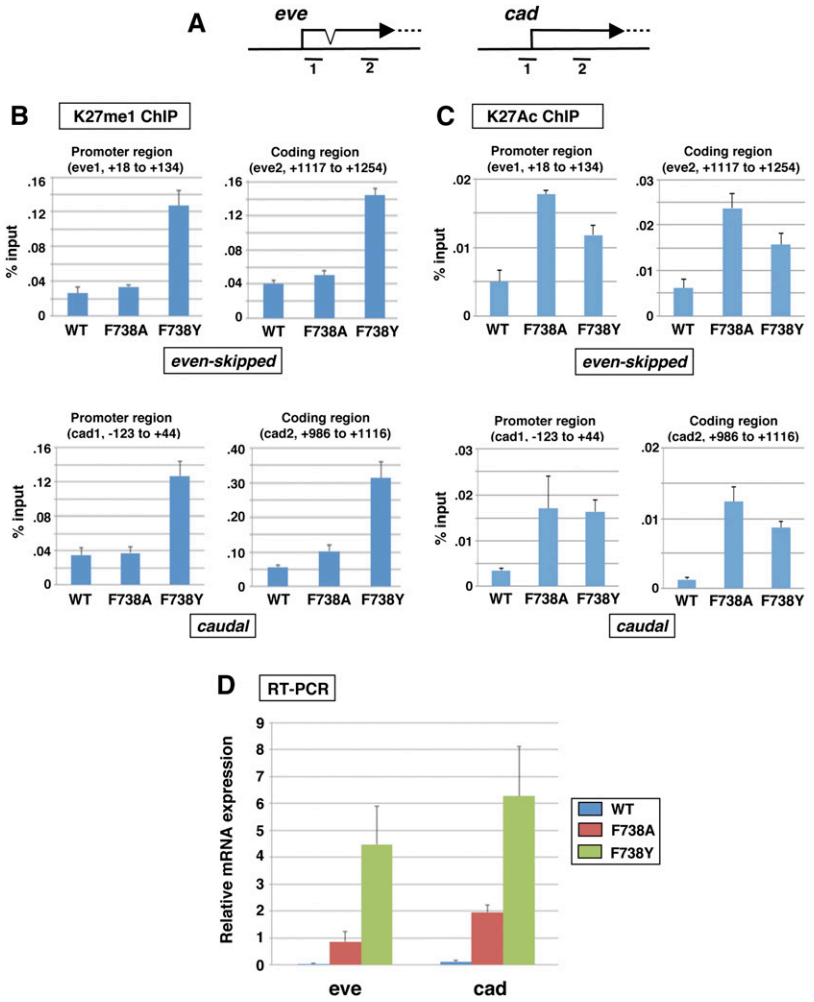

Figure 5 Changes in K27me1, K27Ac, and transcriptional status at target genes after E(Z)-F738Y overexpression. (A) Cartoons depict 5′ portions of the *eve* and *cad* genes spanning the transcription start site regions. Fragments shown below maps represent amplicons used in ChIP assays. Maps are not drawn precisely to scale. (B) ChIP to track H3-K27me1 at indicated locations on the target genes *eve* (top pair of graphs) and *cad* (bottom pair of graphs) after transfection with indicated forms of HA-E(Z). Tested locations are numbered relative to transcription start sites. (C) ChIP to track H3-K27Ac at the same locations tested in (B) and displayed in (A). (D) RT-PCR to track changes in levels of *eve* and *cad* mRNAs. Error bars denote SEM from Q-PCR reactions performed in triplicate.

that an excess of E(Z)-F738Y, incorporated into PRC2, leads to chromatin enriched for H3-K27me1. Additional ChIP experiments revealed that H3-K27 acetylation (K27Ac) levels are also increased at these locations in E(Z)-F738Y–expressing cells (Figure 4E). ChIP to track H3-K27me3 in parallel showed modest declines at *Ubx*, although reduction was not seen at all amplicons tested (Figure S3A).

Excess E(Z)-F738Y leads to target gene desilencing

To assess transcriptional changes that might accompany elevated K27me1, we performed RT-PCR assays on transfected cells (Figure 4F). Cells expressing enzyme-deficient F738A displayed modest *Ubx* desilencing when compared with wild type, consistent with dominant-negative action. However, comparable overexpression of monomethylating F738Y (Figure 4F, inset) led to much more robust desilencing (Figure 4F, red arrow). This desilencing is not maximal, since E(Z) knockdown by RNA interference yields more extreme Ubx activation (Figure 4F, right), but it was reproducibly five- to sevenfold greater than the enzyme-deficient control. This partial desilencing may reflect substantial retention of target gene K27me3 (Figure S3A) at the same time as K27me1 and K27Ac levels rise (Figure 4, D and E).

To assess generality of these findings, we determined chromatin and transcriptional consequences at the *even-skipped* (*eve*) and *caudal* (*cad*) genes, which we verified as additional direct targets of Polycomb silencing in the S2 cells used (Figure S4). As for *Ubx*, ChIP experiments on F738Y- *vs.* F738A-expressing cells revealed elevated K27me1 levels in promoter and gene body regions of these additional targets (Figure 5, A and B). K27Ac levels also increase on *eve* and *cad* (Figure 5C), whereas K27me3 signals on these targets appear reduced or, at certain amplicons, unchanged (Figure S3B). Also, as seen with *Ubx*, RT-PCR assays showed that *eve* and *cad* desilencing is quantitatively more robust with F738Y compared with F738A (Figure 5D and Figure S2B). Taken together, these findings imply that PRC2 engineered to boost K27me1 in target gene chromatin has a positive influence on transcriptional output.

Evidence for in vivo H3-K27 monomethylation independent of PRC2

The results here using fly cells, together with previous work in mammalian cells (Ferrari *et al.* 2014), implies functions for K27 methylation states distinct from repressive me3. Consequently, it is important to fully understand how mono-, di-,

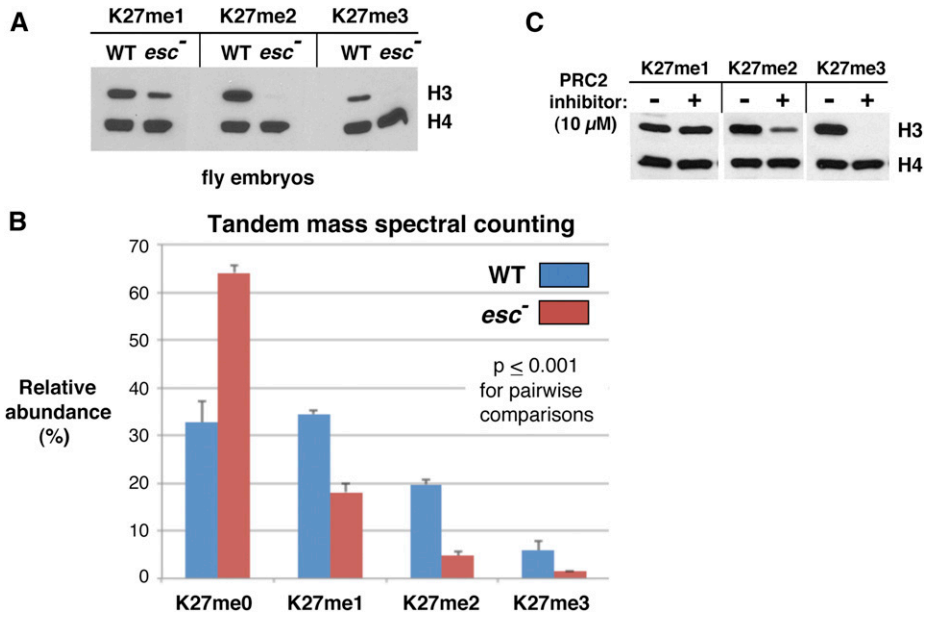

Figure 6 Analyses of H3-K27me1 status after PRC2 disruption in *Drosophila*. (A) Western blots to track bulk H3-K27 methylation in wild-type *vs. esc* mutant *Drosophila* embryos. (B) Tandem mass spectrometric analysis to track H3-K27 methylation states in wild-type *vs. esc* mutant *Drosophila* embryos. Relative abundance of H3/H3.3 peptides spanning residues aa27–40 and bearing indicated K27 modification state is displayed. Error bars denote SEM from mass spectrometric determinations performed in triplicate. Student's *t*-test yielded $P < 0.001$ for all wild-type *vs.* esc mutant pairwise comparisons. (C) Western blots to track bulk H3-K27 methylation in untreated *Drosophila* S2 cells (−) and in cells treated with the PRC2 inhibitor EPZ6438 (+). In (A) and (C), blots were also probed with pan-H4 antibody to assess equivalence of lane loading.

and trimethylated K27 are created and interconverted *in vivo*. Previous experiments suggested that PRC2 was the only K27-targeted methyltransferase in *Drosophila* (Ebert *et al.* 2004). However, in *Arabidopsis* and *Tetrahymena*, methyltransferases wholly distinct from PRC2 have been identified that can modify H3-K27, but their activity is restricted to monomethylation (Jacob *et al.* 2009; Zhang *et al.* 2013).

To further assess the spectrum of possible K27 methyltransferases in *Drosophila*, we tracked bulk accumulation of mono-, di-, and trimethylated H3-K27 in fly embryos and in fly cells where PRC2 activity is eliminated or severely reduced. This is accomplished in embryos by exploiting mutations that remove fly ESC, a PRC2 subunit required for activity *in vitro* and *in vivo* (Struhl 1981; Ketel *et al.* 2005; Nekrasov *et al.* 2005). Flies lacking the *esc* gene survive to adulthood based on the maternal load (Struhl 1981). Interbreeding such *esc*$^-$ adults enables bulk harvesting of embryos that lack both maternal and zygotic gene product, thereby providing PRC2-deficient embryo populations for convenient use in biochemical assays (Ketel *et al.* 2005). We first tracked methylation states by Western blot, which revealed dramatic reductions in overall levels of K27me2 and K27me3 in the *esc*$^-$ fly embryos (Figure 6A). In contrast, substantial K27me1 signal is retained in *esc*$^-$ embryos, suggesting a fraction that is monomethylated independent of PRC2. We also analyzed wild type *vs. esc*$^-$ methylation states via tandem mass spectrometry (see *Materials and Methods*) to obtain a readout that avoids reliance on methylation-specific antibodies. Consistent with above findings, mass spectrometric analysis revealed substantial reduction in K27me2 and K27me3, but retention of about half of the bulk K27me1 in *esc*$^-$ embryos compared to wild type (Figure 6B and Table S1).

As an alternative method for PRC2 disruption, we also analyzed methylation states in fly S2 cells where enzyme activity was inhibited by small molecule interference. After screening a panel of PRC2 inhibitors (Knutson *et al.* 2012; McCabe *et al.* 2012) for impact on fly PRC2 *in vitro*, we determined that EPZ6438 (Knutson *et al.* 2013) provides robust inhibition (Figure S5A). EPZ6438 and its chemically related PRC2 inhibitors work via competition with the SAM methyl donor (Knutson *et al.* 2012, 2013; McCabe *et al.* 2012). Thus, it should block all PRC2-mediated methyl transfer reactions, which was confirmed by *in vitro* HMTase assays of recombinant fly PRC2 (Figure S5, A and B). We then established a regimen for PRC2 inhibition in fly S2 cells, featuring treatment with 10 μM EPZ6438 over 7 days, which eliminates detection of K27me3 by Western blot. Under these conditions of PRC2 inhibition, K27me2 is substantially reduced but still detectable, and K27me1 appears unaffected (Figure 6C). A more quantitative repeat of this PRC2 inhibition experiment reveals that bulk K27me3 is reduced between 16- and 32-fold, and K27me2 is reduced about 10-fold (Figure S6, A and B). In contrast, the level of bulk K27me1 is again, largely unchanged (Figure S6C). Taken together, these findings suggest that substantial amounts of H3-K27 monomethylation can occur in *Drosophila* independent of PRC2.

Discussion

A positive role for H3-K27me1 in transcription

The array of possible chromatin states is amplified by the capacity of histone lysines to bear zero, one, two, or three methyl groups. This reinforces the need to query each methylation state to define their individual impacts on the transcription process. Here, we deployed a PRC2 variant (Figure 2) that primarily catalyzes H3-K27 monomethylation (Figure 3) in an effort to track consequences of altered K27me1 levels at Polycomb targets. Monomethylating E(Z) was made overabundant by transfection into fly S2 cells, leading to several-fold excess of this E(Z)-F738Y compared to endogenous E(Z)

(Figure 4A, top). We found that this boosts K27me1 levels in bulk chromatin (Figure 4A, bottom) and at select target genes (Figure 4D and Figure 5B). We find that genes bearing elevated K27me1 are desilenced to a degree much greater than achieved by comparable overabundance of a generally HMTase-deficient E(Z). Although these experiments do not define stepwise molecular consequences of elevated K27me1, they imply a positive role for this modification in transcription. Thus, K27me1 function is distinct from, and potentially opposed to, the widely recognized role of K27me3 in gene silencing. The association of K27me1 with active transcription is also evident from epigenomics studies in mouse embryonic stem cells (Ferrari *et al.* 2014) and genome-wide distributions in *Drosophila* cells (Figure 1). Previous findings that link fly E(Z) (LaJeunesse and Shearn 1996) or its mammalian orthologs (Shi *et al.* 2007a; Mousavi *et al.* 2012) to positive roles in gene activity could also connect to altered levels of K27me1.

These findings suggest that the number of attached methyl groups on a histone lysine can help dictate active *vs.* repressed chromatin states. Besides the H3-K27 states tracked here, prior studies also associate H3-K9 monomethylation with active genes, whereas K9me2 and K9me3 are highly correlated with repressed chromatin (Barski *et al.* 2007; Wang *et al.* 2008). Another intriguing example is H3-K79, where conversion of the active marks K79me2/3 to K79me1 accompanies Hox gene downregulation in hematopoietic cells, and leukemic transformation is associated with abnormally high K79me2/3 levels via dysfunction of the K79 methyltransferase DOT1 (Deshpande *et al.* 2014). These examples suggest that methyl group addition/subtraction underlies key switches in gene activity and highlight the potential of chemotherapeutic strategies that interconvert target lysine methylations.

Ultimately, manipulation of individual histone methylation states in intact organisms will be needed to fully define functional roles. Indeed, cleverly designed *in vivo* studies validate the key requirement for H3-K27 modification in Polycomb gene silencing (Pengelly *et al.* 2013; McKay *et al.* 2015). However, these approaches, which exploit mutant histone H3 wholly resistant to K27 modification, were not intended to specifically distinguish functions of H3-K27 mono-, di-, and trimethylation. Thus, further work is needed to test engineered PRC2 variants, including E(Z)-F738Y, in transgenic flies. Accomplishing this via CRISPR/Cas-mediated *E(z)* gene conversion would appear straightforward, although conditional expression is likely required because development powered solely by monomethylating PRC2 should be severely compromised.

K36me3, K27me1, and chromatin dynamics during transcription elongation

The K27me1 genomic distribution in *Drosophila* cells (Figure 1), and in mouse embryonic stem cells (Ferrari *et al.* 2014), displays enrichment along gene bodies with peak levels often observed toward 3′ ends. Among other transcription-associated histone modifications, this pattern most closely resembles that of H3-K36me3 (Figure 1; Li *et al.* 2007; Venkatesh and Workman 2013). This implicates K27me1 as one of a suite of chromatin features that track with and/or accumulate in the wake of RNA polymerase II. Besides K36me3, similarly enriched cotranscriptional marks include H3-K79me2/3 and H2B-K120 monoubiquitylation (Tanny 2014; Wu *et al.* 2014). Although functions and interplay of these cotranscriptional modifications are not fully understood, key progress on this has emerged from studies in yeast (Venkatesh and Workman 2015). In particular, Set2, the H3-K36–methylating enzyme, can be recruited to elongating RNA polymerase II via binding to its C-terminal domain repeats bearing phosphorylated serine-2 and serine-5 (Li *et al.* 2003, 2005). Once in place, K36 methylation is implicated in resetting chromatin altered by RNA polymerase II passage; thus, K36me3 suppresses further histone exchange (Venkatesh *et al.* 2012), activates histone deacetylases to restore a hypoacetylated histone state (Carrozza *et al.* 2005; Joshi and Struhl 2005), and promotes re-establishment of regularly spaced nucleosomes by recruiting the ISWI chromatin remodeler as well as CHD1 (Radman-Livaja *et al.* 2012; Smolle *et al.* 2012). Intriguingly, another cotranscriptional remodeler, Kismet (CHD7), promotes K36 methylation in *Drosophila* (Dorighi and Tamkun 2013).

The extent to which these K36me3 functions are conserved in mammalian systems is under investigation. In higher cells, an important cotranscriptional event is histone H3.3 swapping for H3 by the HirA chaperone (Mito *et al.* 2005; Goldberg *et al.* 2010), with regions enriched in K36me displaying a lower H3.3 exchange rate (Kraushaar *et al.* 2013). Thus, a role in suppressing histone turnover in the wake of RNA polymerase II appears conserved. In addition, in higher cells, ZMYND11 is a reader of H3.3-K36me3, where it interacts with other chromatin regulators to influence transcription elongation (Guo *et al.* 2014; Wen *et al.* 2014). Future studies will be needed to reveal if and how K27me1 interfaces with these cotranscriptional players to impact elongation. In particular, the functional connection between K27me1 and K36me3 is supported by frequent coexistence of these marks on the same H3.3 tail and by dependence of gene body K27me1 levels upon activity of K36-methylating enzyme (Ferrari *et al.* 2014). An important goal will be to identify protein "readers" (Taverna *et al.* 2007), which specifically recognize K27me1 and potentially recruit additional chromatin-modifying components. Candidate K27me1 readers might be found among PHD finger proteins, given this domain's ability to distinguish discrete lysine methylation states (Shi *et al.* 2007b).

Potential role of K27me1 in enhancer regions

In addition to gene body enrichment, studies on human hematopoietic cells show that K27me1 can also be enriched at enhancers (Cui *et al.* 2009; Ernst and Kellis 2010; Steiner *et al.* 2011). This is relevant given that a likely impact of the monomethylating PRC2 used here is to boost K27me1 in regions where PRC2 is normally targeted (*i.e.*, Figure 4D and Figure 5B). What regulatory role might K27me1 have

at enhancers and how could this contribute to the desilencing observed here when K27me1 levels are elevated? This might be explained via impacts on K27 acetylation (K27Ac) levels, which genome-wide studies suggest is a signature mark of active enhancers (Creyghton *et al.* 2010; Rada-Iglesias *et al.* 2011). Specifically, whereas H3-K4me1 is identified as a global mark of "primed" enhancers, additional acquisition of H3-K27Ac is implicated in converting enhancers to the active state (Creyghton *et al.* 2010; Rada-Iglesias *et al.* 2011). Thus, the range of possible K27 modification states (K27Ac-K27me0-K27me1-K27me2-K27me3) at enhancers may reflect a range of activity states from on to off. Indeed, there is evidence that K27me3 generally antagonizes K27Ac in fly and mammalian cells (Tie *et al.* 2009; Pasini *et al.* 2010), which makes sense since these are mutually exclusive modifications. More precisely, Ferrari *et al.* (2014) suggest that K27me2 dampens gene activity by preventing K27Ac accumulation at enhancers. In this context, our monomethylating PRC2 could trigger desilencing by shifting the balance away from K27me2/3 at enhancers and toward activating K27Ac. Although we have not tracked defined enhancers, we note that the rise in K27me1 levels at queried targets is accompanied by increased K27Ac (Figure 4E and Figure 5C). Overall, the activating role of K27me1 in coding regions may be coordinated with K36me2/3, whereas at enhancers it may instead impact the balance between K27Ac and K27me2/3.

Machinery for dynamic interconversion of H3-K27 methylation states

PRC2 is the sole H3-K27 methyltransferase identified so far in animal systems and it can perform all three methyl transfer reactions to convert K27me0 to K27me3. In addition, two K27-targeted histone demethylases, Utx and Jmjd3, can remove PRC2-mediated methylation. However, our analyses of fly embryos and cells with PRC2 disrupted (Figure 6) suggest that there are additional enzymes to monomethylate H3-K27. In *esc* mutant embryos, about half of bulk K27me1 is retained whereas K27me2 and me3 are more substantially reduced (Figure 6, A and B). Since these embryos lack PRC2 from fertilization onward, the observed K27me1 is not likely due to transient production of K27me2/3 followed by demethylation. Rather, these results suggest additional methyltransferases, distinct from PRC2, that can monomethylate H3-K27 in chromatin newly assembled after replication. Similarly, PRC2 chemical inhibition in fly cells dramatically reduces K27me2 and me3 levels, but has minimal impact on K27me1 (Figure 6C and Figure S6). Although the mechanics of K27 monomethylation in metazoans has received scant attention, we note that retention of K27me1 after PRC2 disruption has been documented in prior studies using animal cells (Schoeftner *et al.* 2006; Pasini *et al.* 2007; Tie *et al.* 2009; Jung *et al.* 2010; Knutson *et al.* 2012; McCabe *et al.* 2012). These precedents feature PRC2 blockage by a wide variety of chemical or genetic means, including null alleles that remove the mammalian EED or SUZ12 subunits (Schoeftner *et al.* 2006; Pasini *et al.* 2007). Taken together, these findings suggest that K27-specific methyltransferases besides PRC2 may be present in animal systems.

Recently, monomethyltransferases that target H3-K27 have been described in plants and *Tetrahymena* (Jacob *et al.* 2009; Zhang *et al.* 2013). Therefore, these systems are equipped with dedicated enzymes for K27 monomethylation plus PRC2 activity for di- and trimethylation. Furthermore, K27me1 is implicated in DNA replication elongation in *Tetrahymena* (Gao *et al.* 2013) and in replication-coupled heterochromatin maintenance in *Arabidopsis* (Jacob *et al.* 2014), so its functions extend beyond the transcription cycle. Intriguingly, the K27 monomethylating enzymes in these cases interact with the replication processivity factor PCNA (Raynaud *et al.* 2006; Gao *et al.* 2013). However, obvious homologs of these characterized K27 monomethyltransferases, such as ATRX5 and ATRX6 in plants (Jacob *et al.* 2009), appear absent from animal systems based on SET domain-focused searches. Since non-SET HMTases are also possible (Feng *et al.* 2002), biochemical approaches may prove useful as unbiased means to identify any additional K27-methylating enzymes. Thus, further work should assess the full complement of enzymes that control H3-K27 methylation in animals as well as the mechanistic contributions of H3-K27me1 to transcription and other chromatin-based processes.

Acknowledgments

We are grateful to Rick Jones for providing anti-E(Z) and anti-PC antibodies. We thank Marcus Vargas for input on HMTase quantitation and for helpful discussions. This work benefitted from instrumentation and staff support provided by the Center for Mass Spectrometry and Proteomics at the University of Minnesota. This work was supported by National Institutes of Health grants R01 GM049850 to J.A.S. and R35 GM119553 to M.S.

Literature Cited

Baker, K., T. Dhillon, I. Colas, N. Cook, I. Milne *et al.*, 2015 Chromatin state analysis of the barley epigenome reveals a higher-order structure defined by H3K27me1 and H3K27me3 abundance. Plant J. 84: 111–124.

Bannister, A. J., and T. Kouzarides, 2011 Regulation of chromatin by histone modifications. Cell Res. 21: 381–395.

Barrand, S., I. S. Andersen, and P. Collas, 2010 Promoter-exon relationship of H3 lysine 9, 27, 36 and 79 methylation on pluripotency-associated genes. Biochem. Biophys. Res. Commun. 401: 611–617.

Barski, A., S. Cuddapah, K. Cui, T. Y. Roh, D. E. Schones *et al.*, 2007 High-resolution profiling of histone methylations in the human genome. Cell 129: 823–837.

Bell, O., C. Wirbelauer, M. Hild, A. N. Scharf, M. Schwaiger *et al.*, 2007 Localized H3K36 methylation states define histone H4K16 acetylation during transcriptional elongation in *Drosophila*. EMBO J. 26: 4974–4984.

Carrington, E. A., and R. S. Jones, 1996 The Drosophila Enhancer of zeste gene encodes a chromosomal protein: examination of

wild-type and mutant protein distribution. Development 122: 4073–4083.
Carrozza, M. J., B. Li, L. Florens, T. Suganuma, S. K. Swanson *et al.*, 2005 Histone H3 methylation by Set2 directs deacetylation of coding regions by Rpd3S to suppress spurious intragenic transcription. Cell 123: 581–592.
Chan, K. M., D. Fang, H. Gan, R. Hashizume, C. Yu *et al.*, 2013 The histone H3.3K27M mutation in pediatric glioma reprograms H3K27 methylation and gene expression. Genes Dev. 27: 985–990.
Cherbas, L., A. Willingham, D. Zhang, L. Yang, Y. Zou *et al.*, 2011 The transcriptional diversity of 25 *Drosophila* cell lines. Genome Res. 21: 301–314.
Collins, R. E., M. Tachibana, H. Tamaru, K. M. Smith, D. Jia *et al.*, 2005 *In vitro* and *in vivo* analyses of a Phe/Tyr switch controlling product specificity of histone lysine methyltransferases. J. Biol. Chem. 280: 5563–5570.
Couture, J. F., E. Collazo, J. S. Brunzelle, and R. C. Trievel, 2005 Structural and functional analysis of SET8, a histone H4 Lys-20 methyltransferase. Genes Dev. 19: 1455–1465.
Couture, J. F., L. M. Dirk, J. S. Brunzelle, R. L. Houtz, and R. C. Trievel, 2008 Structural origins for the product specificity of SET domain protein methyltransferases. Proc. Natl. Acad. Sci. USA 105: 20659–20664.
Creyghton, M. P., A. W. Cheng, G. G. Welstead, T. Kooistra, B. W. Carey *et al.*, 2010 Histone H3K27ac separates active from poised enhancers and predicts developmental state. Proc. Natl. Acad. Sci. USA 107: 21931–21936.
Cui, K., C. Zang, T. Y. Roh, D. E. Schones, R. W. Childs *et al.*, 2009 Chromatin signatures in multipotent human hematopoietic stem cells indicate the fate of bivalent genes during differentiation. Cell Stem Cell 4: 80–93.
Deshpande, A. J., A. Deshpande, A. U. Sinha, L. Chen, J. Chang *et al.*, 2014 AF10 regulates progressive H3K79 methylation and HOX gene expression in diverse AML subtypes. Cancer Cell 26: 896–908.
Dorighi, K. M., and J. W. Tamkun, 2013 The trithorax group proteins Kismet and ASH1 promote H3K36 dimethylation to counteract Polycomb group repression in *Drosophila*. Development 140: 4182–4192.
Ebert, A., G. Schotta, S. Lein, S. Kubicek, V. Krauss *et al.*, 2004 Su(var) genes regulate the balance between euchromatin and heterochromatin in *Drosophila*. Genes Dev. 18: 2973–2983.
Ernst, J., and M. Kellis, 2010 Discovery and characterization of chromatin states for systematic annotation of the human genome. Nat. Biotechnol. 28: 817–825.
Feng, Q., H. Wang, H. H. Ng, H. Erdjument-Bromage, P. Tempst *et al.*, 2002 Methylation of H3-lysine 79 is mediated by a new family of HMTases without a SET domain. Curr. Biol. 12: 1052–1058.
Ferrari, K. J., A. Scelfo, S. Jammula, A. Cuomo, I. Barozzi *et al.*, 2014 Polycomb-dependent H3K27me1 and H3K27me2 regulate active transcription and enhancer fidelity. Mol. Cell 53: 49–62.
Frei, E., D. Bopp, M. Burri, S. Baumgartner, J. E. Edström *et al.*, 1985 Isolation and structural analysis of the extra sex combs gene of *Drosophila*. Cold Spring Harb. Symp. Quant. Biol. 50: 127–134.
Gao, S., J. Xiong, C. Zhang, B. R. Berquist, R. Yang *et al.*, 2013 Impaired replication elongation in *Tetrahymena* mutants deficient in histone H3 Lys 27 monomethylation. Genes Dev. 27: 1662–1679.
Goldberg, A. D., L. A. Banaszynski, K. M. Noh, P. W. Lewis, S. J. Elsaesser *et al.*, 2010 Distinct factors control histone variant H3.3 localization at specific genomic regions. Cell 140: 678–691.
Guo, R., L. Zheng, J. W. Park, R. Lv, H. Chen *et al.*, 2014 BS69/ZMYND11 reads and connects histone H3.3 lysine 36 trimethylation-decorated chromatin to regulated pre-mRNA processing. Mol. Cell 56: 298–310.
Heintzman, N. D., R. K. Stuart, G. Hon, Y. Fu, C. W. Ching *et al.*, 2007 Distinct and predictive chromatin signatures of transcriptional promoters and enhancers in the human genome. Nat. Genet. 39: 311–318.
Heintzman, N. D., G. C. Hon, R. D. Hawkins, P. Kheradpour, A. Stark *et al.*, 2009 Histone modifications at human enhancers reflect global cell-type-specific gene expression. Nature 459: 108–112.
Herz, H. M., M. Mohan, A. S. Garruss, K. Liang, Y. H. Takahashi *et al.*, 2012 Enhancer-associated H3K4 monomethylation by Trithorax-related, the *Drosophila* homolog of mammalian Mll3/Mll4. Genes Dev. 26: 2604–2620.
Jacob, Y., S. Feng, C. A. LeBlanc, Y. V. Bernatavichute, H. Stroud *et al.*, 2009 ATXR5 and ATXR6 are H3K27 monomethyltransferases required for chromatin structure and gene silencing. Nat. Struct. Mol. Biol. 16: 763–768.
Jacob, Y., E. Bergamin, M. T. Donoghue, V. Mongeon, C. LeBlanc *et al.*, 2014 Selective methylation of histone H3 variant H3.1 regulates heterochromatin replication. Science 343: 1249–1253.
Jones, C. A., J. Ng, A. J. Peterson, K. Morgan, J. Simon *et al.*, 1998 The *Drosophila* esc and E(z) proteins are direct partners in polycomb group-mediated repression. Mol. Cell. Biol. 18: 2825–2834.
Joshi, A. A., and K. Struhl, 2005 Eaf3 chromodomain interaction with methylated H3–K36 links histone deacetylation to Pol II elongation. Mol. Cell 20: 971–978.
Joshi, P., E. A. Carrington, L. Wang, C. S. Ketel, E. L. Miller *et al.*, 2008 Dominant alleles identify SET domain residues required for histone methyltransferase of Polycomb repressive complex 2. J. Biol. Chem. 283: 27757–27766.
Jung, H. R., D. Pasini, K. Helin, and O. N. Jensen, 2010 Quantitative mass spectrometry of histones H3.2 and H3.3 in Suz12-deficient mouse embryonic stem cells reveals distinct, dynamic post-translational modifications at Lys-27 and Lys-36. Mol. Cell. Proteomics 9: 838–850.
Ketel, C. S., E. F. Andersen, M. L. Vargas, J. Suh, S. Strome *et al.*, 2005 Subunit contributions to histone methyltransferase activities of fly and worm polycomb group complexes. Mol. Cell. Biol. 25: 6857–6868.
Kharchenko, P. V., A. A. Alekseyenko, Y. B. Schwartz, A. Minoda, N. C. Riddle *et al.*, 2011 Comprehensive analysis of the chromatin landscape in *Drosophila melanogaster*. Nature 471: 480–485.
Kim, K. H., and C. W. Roberts, 2016 Targeting EZH2 in cancer. Nat. Med. 22: 128–134.
Klose, R. J., and Y. Zhang, 2007 Regulation of histone methylation by demethylimination and demethylation. Nat. Rev. Mol. Cell Biol. 8: 307–318.
Knutson, S. K., T. J. Wigle, N. M. Warholic, C. J. Sneeringer, C. J. Allain *et al.*, 2012 A selective inhibitor of EZH2 blocks H3K27 methylation and kills mutant lymphoma cells. Nat. Chem. Biol. 8: 890–896.
Knutson, S. K., N. M. Warholic, T. J. Wigle, C. R. Klaus, C. J. Allain *et al.*, 2013 Durable tumor regression in genetically altered malignant rhabdoid tumors by inhibition of methyltransferase EZH2. Proc. Natl. Acad. Sci. USA 110: 7922–7927.
Kraushaar, D. C., W. Jin, A. Maunakea, B. Abraham, M. Ha *et al.*, 2013 Genome-wide incorporation dynamics reveal distinct categories of turnover for the histone variant H3.3. Genome Biol. 14: R121.
LaJeunesse, D., and A. Shearn, 1996 E(z): a polycomb group gene or a trithorax group gene? Development 122: 2189–2197.

Levenstein, M. E., and J. T. Kadonaga, 2002 Biochemical analysis of chromatin containing recombinant *Drosophila* core histones. J. Biol. Chem. 277: 8749–8754.
Lewis, P. W., M. M. Muller, M. S. Koletsky, F. Cordero, S. Lin *et al.*, 2013 Inhibition of PRC2 activity by a gain-of-function H3 mutation found in pediatric glioblastoma. Science 340: 857–861.
Li, B., L. Howe, S. Anderson, J. R. Yates, III, and J. L. Workman, 2003 The Set2 histone methyltransferase functions through the phosphorylated carboxyl-terminal domain of RNA polymerase II. J. Biol. Chem. 278: 8897–8903.
Li, B., M. Carey, and J. L. Workman, 2007 The role of chromatin during transcription. Cell 128: 707–719.
Li, M., H. P. Phatnani, Z. Guan, H. Sage, A. L. Greenleaf *et al.*, 2005 Solution structure of the Set2-Rpb1 interacting domain of human Set2 and its interaction with the hyperphosphorylated C-terminal domain of Rpb1. Proc. Natl. Acad. Sci. USA 102: 17636–17641.
Lin-Moshier, Y., P. J. Sebastian, L. Higgins, N. D. Sampson, J. E. Hewitt *et al.*, 2013 Re-evaluation of the role of calcium homeostasis endoplasmic reticulum protein (CHERP) in cellular calcium signaling. J. Biol. Chem. 288: 355–367.
Liu, T., J. A. Ortiz, L. Taing, C. A. Meyer, B. Lee *et al.*, 2011a Cistrome: an integrative platform for transcriptional regulation studies. Genome Biol. 12: R83.
Liu, T., A. Rechtsteiner, T. A. Egelhofer, A. Vielle, I. Latorre *et al.*, 2011b Broad chromosomal domains of histone modification patterns in *C. elegans*. Genome Res. 21: 227–236.
Margueron, R., and D. Reinberg, 2011 The Polycomb complex PRC2 and its mark in life. Nature 469: 343–349.
McCabe, M. T., H. M. Ott, G. Ganji, S. Korenchuk, C. Thompson *et al.*, 2012 EZH2 inhibition as a therapeutic strategy for lymphoma with EZH2-activating mutations. Nature 492: 108–112.
McKay, D. J., S. Klusza, T. J. Penke, M. P. Meers, K. P. Curry *et al.*, 2015 Interrogating the function of metazoan histones using engineered gene clusters. Dev. Cell 32: 373–386.
Mito, Y., J. G. Henikoff, and S. Henikoff, 2005 Genome-scale profiling of histone H3.3 replacement patterns. Nat. Genet. 37: 1090–1097.
Mousavi, K., H. Zare, A. H. Wang, and V. Sartorelli, 2012 Polycomb protein Ezh1 promotes RNA polymerase II elongation. Mol. Cell 45: 255–262.
Muller, J., C. M. Hart, N. J. Francis, M. L. Vargas, A. Sengupta *et al.*, 2002 Histone methyltransferase activity of a *Drosophila* Polycomb group repressor complex. Cell 111: 197–208.
Nekrasov, M., B. Wild, and J. Muller, 2005 Nucleosome binding and histone methyltransferase activity of *Drosophila* PRC2. EMBO Rep. 6: 348–353.
Nekrasov, M., T. Klymenko, S. Fraterman, B. Papp, K. Oktaba *et al.*, 2007 Pcl-PRC2 is needed to generate high levels of H3–K27 trimethylation at Polycomb target genes. EMBO J. 26: 4078–4088.
Pasini, D., A. P. Bracken, J. B. Hansen, M. Capillo, and K. Helin, 2007 The polycomb group protein Suz12 is required for embryonic stem cell differentiation. Mol. Cell. Biol. 27: 3769–3779.
Pasini, D., M. Malatesta, H. R. Jung, J. Walfridsson, A. Willer *et al.*, 2010 Characterization of an antagonistic switch between histone H3 lysine 27 methylation and acetylation in the transcriptional regulation of Polycomb group target genes. Nucleic Acids Res. 38: 4958–4969.
Pengelly, A. R., O. Copur, H. Jackle, A. Herzig, and J. Muller, 2013 A histone mutant reproduces the phenotype caused by loss of histone-modifying factor Polycomb. Science 339: 698–699.
Pereira, C. F., F. M. Piccolo, T. Tsubouchi, S. Sauer, N. K. Ryan *et al.*, 2010 ESCs require PRC2 to direct the successful reprogramming of differentiated cells toward pluripotency. Cell Stem Cell 6: 547–556.
Peters, A. H., S. Kubicek, K. Mechtler, R. J. O'Sullivan, A. A. Derijck *et al.*, 2003 Partitioning and plasticity of repressive histone methylation states in mammalian chromatin. Mol. Cell 12: 1577–1589.
Rada-Iglesias, A., R. Bajpai, T. Swigut, S. A. Brugmann, R. A. Flynn *et al.*, 2011 A unique chromatin signature uncovers early developmental enhancers in humans. Nature 470: 279–283.
Radman-Livaja, M., T. K. Quan, L. Valenzuela, J. A. Armstrong, T. van Welsem *et al.*, 2012 A key role for Chd1 in histone H3 dynamics at the 3′ ends of long genes in yeast. PLoS Genet. 8: e1002811.
Rai, A. N., M. L. Vargas, L. Wang, E. F. Andersen, E. L. Miller *et al.*, 2013 Elements of the polycomb repressor SU(Z)12 needed for histone H3–K27 methylation, the interface with E(Z), and *in vivo* function. Mol. Cell. Biol. 33: 4844–4856.
Rappsilber, J., Y. Ishihama, and M. Mann, 2003 Stop and go extraction tips for matrix-assisted laser desorption/ionization, nanoelectrospray, and LC/MS sample pretreatment in proteomics. Anal. Chem. 75: 663–670.
Raynaud, C., R. Sozzani, N. Glab, S. Domenichini, C. Perennes *et al.*, 2006 Two cell-cycle regulated SET-domain proteins interact with proliferating cell nuclear antigen (PCNA) in Arabidopsis. Plant J. 47: 395–407.
Roudier, F., I. Ahmed, C. Berard, A. Sarazin, T. Mary-Huard *et al.*, 2011 Integrative epigenomic mapping defines four main chromatin states in Arabidopsis. EMBO J. 30: 1928–1938.
Sathe, S. S., and P. J. Harte, 1995 The *Drosophila extra sex combs* protein contains WD motifs essential for its function as a repressor of homeotic genes. Mech. Dev. 52: 77–87.
Sawarkar, R., and R. Paro, 2010 Interpretation of developmental signaling at chromatin: the Polycomb perspective. Dev. Cell 19: 651–661.
Schoeftner, S., A. K. Sengupta, S. Kubicek, K. Mechtler, L. Spahn *et al.*, 2006 Recruitment of PRC1 function at the initiation of X inactivation independent of PRC2 and silencing. EMBO J. 25: 3110–3122.
Shi, B., J. Liang, X. Yang, Y. Wang, Y. Zhao *et al.*, 2007a Integration of estrogen and Wnt signaling circuits by the polycomb group protein EZH2 in breast cancer cells. Mol. Cell. Biol. 27: 5105–5119.
Shi, X., I. Kachirskaia, K. L. Walter, J. H. Kuo, A. Lake *et al.*, 2007b Proteome-wide analysis in *Saccharomyces cerevisiae* identifies several PHD fingers as novel direct and selective binding modules of histone H3 methylated at either lysine 4 or lysine 36. J. Biol. Chem. 282: 2450–2455.
Shin, H., T. Liu, A. K. Manrai, and X. S. Liu, 2009 CEAS: *cis*-regulatory element annotation system. Bioinformatics 25: 2605–2606.
Simon, J. A., and R. E. Kingston, 2013 Occupying chromatin: Polycomb mechanisms for getting to genomic targets, stopping transcriptional traffic, and staying put. Mol. Cell 49: 808–824.
Simon, J. A., and C. A. Lange, 2008 Roles of the EZH2 histone methyltransferase in cancer epigenetics. Mutat. Res. 647: 21–29.
Smolle, M., S. Venkatesh, M. M. Gogol, H. Li, Y. Zhang *et al.*, 2012 Chromatin remodelers Isw1 and Chd1 maintain chromatin structure during transcription by preventing histone exchange. Nat. Struct. Mol. Biol. 19: 884–892.
Steiner, L. A., V. P. Schulz, Y. Maksimova, C. Wong, and P. G. Gallagher, 2011 Patterns of histone H3 lysine 27 monomethylation and erythroid cell type-specific gene expression. J. Biol. Chem. 286: 39457–39465.
Struhl, G., 1981 A gene product required for correct initiation of segmental determination in *Drosophila*. Nature 293: 36–41.
Surface, L. E., S. R. Thornton, and L. A. Boyer, 2010 Polycomb group proteins set the stage for early lineage commitment. Cell Stem Cell 7: 288–298.

Tanny, J. C., 2014 Chromatin modification by the RNA polymerase II elongation complex. Transcription 5: e988093.
Taverna, S. D., H. Li, A. J. Ruthenburg, C. D. Allis, and D. J. Patel, 2007 How chromatin-binding modules interpret histone modifications: lessons from professional pocket pickers. Nat. Struct. Mol. Biol. 14: 1025–1040.
Tie, F., R. Banerjee, C. A. Stratton, J. Prasad-Sinha, V. Stepanik *et al.*, 2009 CBP-mediated acetylation of histone H3 lysine 27 antagonizes *Drosophila* Polycomb silencing. Development 136: 3131–3141.
Venkatesh, S., and J. L. Workman, 2013 Set2 mediated H3 lysine 36 methylation: regulation of transcription elongation and implications in organismal development. Wiley Interdiscip. Rev. Dev. Biol. 2: 685–700.
Venkatesh, S., and J. L. Workman, 2015 Histone exchange, chromatin structure and the regulation of transcription. Nat. Rev. Mol. Cell Biol. 16: 178–189.
Venkatesh, S., M. Smolle, H. Li, M. M. Gogol, M. Saint *et al.*, 2012 Set2 methylation of histone H3 lysine 36 suppresses histone exchange on transcribed genes. Nature 489: 452–455.
Wang, L., J. L. Brown, R. Cao, Y. Zhang, J. A. Kassis *et al.*, 2004 Hierarchical recruitment of polycomb group silencing complexes. Mol. Cell 14: 637–646.
Wang, L., N. Jahren, M. L. Vargas, E. F. Andersen, J. Benes *et al.*, 2006 Alternative ESC and ESC-like subunits of a polycomb group histone methyltransferase complex are differentially deployed during *Drosophila* development. Mol. Cell. Biol. 26: 2637–2647.
Wang, L., N. Jahren, E. L. Miller, C. S. Ketel, D. R. Mallin *et al.*, 2010 Comparative analysis of chromatin binding by Sex Comb on Midleg (SCM) and other polycomb group repressors at a *Drosophila Hox* gene. Mol. Cell. Biol. 30: 2584–2593.
Wang, Z., C. Zang, J. A. Rosenfeld, D. E. Schones, A. Barski *et al.*, 2008 Combinatorial patterns of histone acetylations and methylations in the human genome. Nat. Genet. 40: 897–903.
Wen, H., Y. Li, Y. Xi, S. Jiang, S. Stratton *et al.*, 2014 ZMYND11 links histone H3.3K36me3 to transcription elongation and tumour suppression. Nature 508: 263–268.
Wu, L., L. Li, B. Zhou, Z. Qin, and Y. Dou, 2014 H2B ubiquitylation promotes RNA Pol II processivity via PAF1 and pTEFb. Mol. Cell 54: 920–931.
Xie, H., J. Xu, J. H. Hsu, M. Nguyen, Y. Fujiwara *et al.*, 2014 Polycomb repressive complex 2 regulates normal hematopoietic stem cell function in a developmental-stage-specific manner. Cell Stem Cell 14: 68–80.
Zentner, G. E., and S. Henikoff, 2013 Regulation of nucleosome dynamics by histone modifications. Nat. Struct. Mol. Biol. 20: 259–266.
Zhang, C., A. J. Molascon, S. Gao, Y. Liu, and P. C. Andrews, 2013 Quantitative proteomics reveals that the specific methyltransferases Txr1p and Ezl2p differentially affect the mono-, di- and trimethylation states of histone H3 lysine 27 (H3K27). Mol. Cell. Proteomics 12: 1678–1688.
Zhang, X., Z. Yang, S. I. Khan, J. R. Horton, H. Tamaru *et al.*, 2003 Structural basis for the product specificity of histone lysine methyltransferases. Mol. Cell 12: 177–185.

Communicating editor: P. Geyer